

Subgrid-scale model for the temperature fluctuations in reacting hypersonic turbulent flows

M. Pino Martín and Graham V. Candler^{a)}

Department of Aerospace Engineering and Mechanics, University of Minnesota, 110 Union St. SE, Minneapolis, Minnesota 55455

(Received 6 January 1999; accepted 23 April 1999)

A direct numerical simulation (DNS) database is used to develop a model of subgrid-scale temperature fluctuations for use in large-eddy simulations of turbulent, reacting hypersonic flows. The proposed model uses a probability density representation of the temperature fluctuations. The DNS database reveals a physically consistent relation between the resolved-scale flow conditions that may be used to predict the standard deviation of the Gaussian probability density function (PDF). The model is calibrated and tested by comparison to simulations of decaying isotropic turbulence. The conditional single-variable PDF model is found to capture the fluctuations in temperature and product formation. © 1999 American Institute of Physics. [S1070-6631(99)01909-1]

INTRODUCTION

The boundary layer on proposed air-breathing hypersonic cruise vehicles will be turbulent and chemically reacting. To aid the design of such vehicles, a greater understanding of turbulent hypersonic flows is needed. Direct numerical simulations (DNS) of hypersonic flows at realistic Reynolds numbers are very costly. For this reason large-eddy simulations (LES) of these flows are more attractive. Therefore, subgrid-scale (SGS) models need to be devised to represent the turbulence-chemistry interaction in LES of hypersonic flows.

Much work has been done on the modeling of turbulent reacting flows.¹⁻¹⁰ However, most of this work has been focused on combustion related applications, where fluctuations in the chemical source term are mainly caused by fluctuations in the species concentrations. In hypersonic flows, the equilibrium composition of reacting air depends strongly on the temperature. Furthermore, the reactions are temperature limited and the reaction rate depends exponentially on temperature. With the very high energies present in hypersonic flows, the temperature fluctuations will be large, and result in variations in the reaction rates. Therefore, in hypersonic flows the temperature fluctuations must be modeled to obtain accurate rates of reaction and product formation.

In LES, it is generally assumed that the small scales are more isotropic and more universal in character for different flows than the large scales. Therefore, it is customary to develop and test SGS models in isotropic turbulence, for later use and refinement in the more complex flows. In our previous work,¹¹ we studied the interaction between decaying isotropic turbulence and finite-rate chemical reactions at conditions typical of a hypersonic boundary layer. The results confirmed that the interaction is characterized by the increased or decreased magnitude of the temperature fluctuations for exothermic or endothermic reactions, respectively.

In this paper, we use the DNS database of isotropic reacting turbulence to develop and evaluate a model for the temperature fluctuations. As reactions, we use either dissociating nitrogen molecules or dissociating oxygen molecules. These are the primary reactions that occur in hypersonic boundary layers. Our approach builds on the reaction rate modeling for combustion applications. In particular, Gaffney *et al.*⁷ assume a probability density function (PDF) for the temperature fluctuations and investigate how the fluctuations affect the combustion process. The proposed model has a similar form, however we use the results of DNS to calibrate the model. Therefore, the parameters that describe the PDF are based on resolved-scale turbulence data. This model represents the unresolved (subgrid-scale) fluctuations for use in large-eddy simulations of turbulence, where the small scales are assumed to be isotropic.

In the remainder of the paper, we review the governing equations, we Favre average these equations and show that the unresolved temperature fluctuations must be modeled for large-eddy simulations. We then discuss the data analysis for the prediction of the temperature fluctuations, and evaluate the model by comparison with the DNS results.

GOVERNING EQUATIONS

The equations describing the unsteady motion of a reacting flow with no contribution of vibrational modes are given by the species mass, mass-averaged momentum, and total energy conservation equations

$$\frac{\partial \rho_s}{\partial t} + \frac{\partial}{\partial x_j} (\rho_s u_j + \rho_s v_{sj}) = w_s,$$

$$\frac{\partial \rho u_i}{\partial t} + \frac{\partial}{\partial x_j} (\rho u_i u_j + p \delta_{ij} - \sigma_{ij}) = 0,$$

$$\frac{\partial E}{\partial t} + \frac{\partial}{\partial x_j} \left((E+p)u_j - u_i \sigma_{ij} + q_j + \sum_s \rho_s v_{sj} h_s \right) = 0, \quad (1)$$

^{a)}Electronic mail: candler@aem.umn.edu

where ρ_s is the density of species s ; w_s represents the rate of production of species s due to chemical reactions; ρ_s is the density of species s ; u_j is the mass-averaged velocity in the j direction; $v_{s,j}$ is the diffusion velocity of species s ; ρ is the sum over species s density; p is the pressure; σ_{ij} is the shear stress tensor given by a linear stress-strain relationship; q_j is the heat flux due to temperature gradients; h_s is the specific enthalpy of species s ; and E is the total energy per unit volume given by

$$E = \sum_s \rho_s c_{vs} T + \frac{1}{2} \rho u_i u_i + \sum_s \rho_s h_s^\circ, \quad (2)$$

where c_{vs} is the specific heat at constant volume of species s ; and h_s° represents the heat of formation of species s .

We consider a simple reaction system: Dissociation of diatomic molecules. This is the primary reaction that occurs in hypersonic boundary layers, and it serves as a good example for the form of the chemical source term. The nitrogen dissociation reaction may be written symbolically as



where M represents a collision partner, which is either N_2 or N in this case. The source term for N_2 can be written using the law of mass action

$$w_{\text{N}_2} = -M_{\text{N}_2} k_f \left(\frac{\rho_{\text{N}_2}}{M_{\text{N}_2}} \right) \left(\frac{\rho_{\text{N}_2}}{M_{\text{N}_2}} + \frac{\rho_{\text{N}}}{M_{\text{N}}} \right) + M_{\text{N}_2} k_b \left(\frac{\rho_{\text{N}}}{M_{\text{N}}} \right)^2 \left(\frac{\rho_{\text{N}_2}}{M_{\text{N}_2}} + \frac{\rho_{\text{N}}}{M_{\text{N}}} \right) = w_{f\text{N}_2} + w_{b\text{N}_2}, \quad (4)$$

and $w_{\text{N}_2} = -w_{\text{N}}$. k_f and k_b are the forward and backward reaction rates, respectively; these are written as

$$k_f = CT^\eta e^{-\theta/T}, \quad (5)$$

$$k_b = \frac{k_f}{K_{eq}},$$

where C , η , and θ are experimentally determined constants,¹² and K_{eq} is the known temperature-dependent equilibrium constant.¹²

For a two-species mixture, the diffusion velocity can be accurately represented using Fick's law

$$\rho_s v_{s,j} = -\rho D \frac{\partial c_s}{\partial x_j}, \quad (6)$$

where $c_s = \rho_s / \rho$ is the mass fraction, and D is the diffusion coefficient given in terms of the Lewis number

$$Le = \frac{\rho D Pr}{\mu}, \quad (7)$$

where Pr is the Prandtl number, μ is the viscosity, and Le is taken to be unity, so that the energy transport due to mass diffusion is equal to the energy transport due to thermal conduction.

FAVRE-FILTERING OF CONSERVATION EQUATIONS

To discuss how the conservation equations must be modeled, we need to separate the resolvable fluctuations from those that the grid cannot resolve. In compressible flows, it is suitable to use Favre-filtering to avoid the introduction of subgrid-scale terms in the equation of conservation of mass. A Favre-filtered variable is defined as $\tilde{f} = (\overline{\rho f}) / \bar{\rho}$, where the over-bar denotes a filtering operation that maintains only the large scales. Accordingly, the Favre-filtered forms of the species mass, momentum, and total energy equations are

$$\begin{aligned} \frac{\partial}{\partial t} (\bar{\rho}_s) + \frac{\partial}{\partial x_j} (\bar{\rho} \tilde{c}_s \tilde{u}_j + \bar{\rho} \tilde{v}_{s,j} + V_{s,j}) &= \bar{w}_s, \\ \frac{\partial}{\partial t} (\bar{\rho} \tilde{u}_i) + \frac{\partial}{\partial x_j} (\bar{\rho} \tilde{u}_i \tilde{u}_j + \bar{p} \delta_{ij} + \tau_{ij} - \tilde{\sigma}_{ij}) &= 0, \\ \frac{\partial \tilde{E}}{\partial t} + \frac{\partial}{\partial x_j} \left((\tilde{E} + \bar{p}) \tilde{u}_j - \tilde{\sigma}_{ij} \tilde{u}_j + \tilde{q}_j + \bar{p} \sum_s \tilde{c}_s \tilde{v}_{s,j} \tilde{h}_s \right. \\ &\quad \left. + \gamma \tilde{c}_v Q_j + \Sigma_j + \sum_s h_s^\circ V_{s,j} \right) = 0, \end{aligned} \quad (8)$$

where $\tilde{c}_s = \bar{\rho}_s / \bar{\rho}$ is the Favre-averaged mass fraction, and the SGS diffusion velocity of species has been introduced

$$V_{s,j} = \bar{\rho} (\widetilde{c_s u_j} - \tilde{c}_s \tilde{u}_j). \quad (9)$$

In the momentum equation, τ_{ij} is the SGS stress

$$\tau_{ij} = \bar{\rho} (\widetilde{u_i u_j} - \tilde{u}_i \tilde{u}_j), \quad (10)$$

and $\tilde{\sigma}_{ij}$ has been simplified according to

$$\tilde{\sigma}_{ij} = \tilde{\mu} \frac{\partial \tilde{u}_i}{\partial x_j} + \tilde{\mu} \frac{\partial \tilde{u}_j}{\partial x_i} - \frac{2}{3} \tilde{\mu} \frac{\partial \tilde{u}_k}{\partial x_k} \delta_{ij}, \quad (11)$$

thus, the viscosity is assumed to be a weak function of the mixture mole fractions, and its fluctuations are neglected. In the energy equation, we have introduced the average specific heats, \tilde{c}_v , the SGS heat flux

$$Q_j = \bar{\rho} (\widetilde{u_j T} - \tilde{u}_j \tilde{T}), \quad (12)$$

and the SGS kinetic-energy flux

$$\Sigma_j = \frac{\bar{\rho}}{2} (\widetilde{u_k u_k u_j} - \tilde{u}_k \tilde{u}_k \tilde{u}_j). \quad (13)$$

These terms are derived by considering the Favre average of the energy-velocity product

$$\begin{aligned} \widetilde{E u_j} &= \bar{\rho} \Sigma_s c_{vs} \widetilde{c_s u_j T} + \frac{1}{2} \bar{\rho} \widetilde{u_k u_k u_j} + \bar{\rho} \Sigma_s h^\circ \widetilde{c_s u_j} \\ &= \tilde{E} \tilde{u}_j + \Sigma_j + \Sigma_s h_s^\circ V_{s,j} + \bar{\rho} \Sigma_s c_{vs} (\widetilde{c_s T u_j} - \tilde{c}_s \tilde{T} \tilde{u}_j) \\ &\approx \tilde{E} \tilde{u}_j + \tilde{c}_v Q_j + \Sigma_j + \Sigma_s h_s^\circ V_{s,j}, \end{aligned} \quad (14)$$

where we have assumed that the mass fraction fluctuations are not directly correlated with the temperature-velocity variations. This assumption is well founded in the flows of interest, since, as observed in the DNS results, the effect of the mass fraction fluctuations on the reaction rate is negligible compared to the effect of the temperature fluctuations. The energy gives the temperature

$$\tilde{E} = \bar{\rho} \tilde{c}_v \tilde{T} + \frac{1}{2} \bar{\rho} \tilde{u}_i \tilde{u}_i + \bar{\rho} \Sigma_s h_s^o \tilde{c}_s + \bar{\rho} \Sigma_s c_{vs} \Phi_s + \frac{1}{2} \tau_{ij}, \quad (15)$$

where $\Phi_s = \widetilde{Tc_s} - \tilde{T} \tilde{c}_s$. And the pressure is given by

$$\bar{p} = \bar{\rho} R \tilde{T} + \bar{\rho} R \Sigma_s \Phi_s. \quad (16)$$

The results from DNS of isotropic turbulence show that the terms involving the SGS temperature-species correlation, Φ_s , are negligible in comparison to the rest of the terms in the equations of state and total energy.

Finally, we must consider the chemical source term, \bar{w}_s , in the continuity equation. The strong temperature dependence of the source term can be seen by representing the variables as their filtered and subgrid-scale values: $T = \bar{T} + T'$ and $c_s = \bar{c}_s + c'_s$. The source term (4) to first order in the subgrid-scale quantities is

$$w_{fN_2} = \bar{w}_{fN_2} + \bar{w}_{fN_2} \left(\left(\frac{\theta}{\bar{T}} + \eta \right) \frac{T'}{\bar{T}} + c'_{N_2} \right) + \dots, \quad (17)$$

$$w_{bN_2} = \bar{w}_{bN_2} + \bar{w}_{bN_2} \left(\left(\frac{\theta}{\bar{T}} + \eta \right) \frac{T'}{\bar{T}} - 2c'_{N_2} \right) + \dots,$$

where $\bar{w} = w(\bar{T})$. We have also made use of the fact that $c'_{N_2} = -c'_{O_2}$, and we have assumed that the variation of K_{eq} in temperature is relatively weak, which is a good approximation at high temperatures. The variations of w_{N_2} caused by temperature fluctuations may be especially large because θ is typically an order of magnitude larger than the temperature. Thus, to obtain accurate \bar{w}_s we must model the subgrid-scale temperature fluctuations for use in Eqs. (4) and (5).

This derivation shows that the following terms must be modeled:

$$\begin{aligned} V_{sj} &= \text{SGS diffusion of species } s, \\ \tau_{ij} &= \text{SGS stress}, \\ Q_j &= \text{SGS heat flux}, \\ \Sigma_j &= \text{SGS kinetic-energy flux}, \\ T^{\text{sgs}} &= \text{SGS temperature fluctuations}. \end{aligned} \quad (18)$$

Much work has been done in modeling τ_{ij} and Q_j ,^{13–18} although less effort has been given to modeling V_{sj} , Σ_j , and T^{sgs} . Gao and O'Brien¹⁸ briefly discuss the modeling of V_{sj} in the context of a dynamic SGS model, and Réveillon and Vervisch¹⁹ discuss the modeling of Σ_j . Recently Martín *et al.*²⁰ have tested dynamic and mixed models for the various terms appearing in the total energy equation in compressible, nonreacting isotropic turbulent flow. The current paper includes the development of a model for the temperature fluctuations in reacting turbulence.

SIMULATIONS OF REACTING TURBULENCE

In this section we present the numerical simulations for three-dimensional, compressible, homogeneous, isotropic, reacting turbulent flow. We use the same numerical method and isotropic initialization as Martín and Candler.¹¹ In particular, we use a sixth-order accurate finite difference

scheme,²¹ and a fourth-order accurate Runge–Kutta time integration. The simulations are performed on grids with 128³ points. The fluctuating fields are initialized using Ristorcelli and Blaisdell²² consistent initial conditions.

The nondimensional parameters¹¹ governing the turbulence–chemistry interaction are the turbulent Reynolds number, the Mach number, the Damköhler number, and the relative heat release, namely

$$M_t = \frac{q}{a}, \quad Re_\lambda = \frac{\rho u' \lambda}{\mu}, \quad (19)$$

$$Da = \frac{\tau_t}{\tau_c}, \quad \overline{\Delta h^o} = -\frac{\Delta h^o}{c_v T + (1/2)q^2},$$

where the chemical time scale, $\tau_c = \rho / |w \log(K_{eq})|$, is different from the definition given in Martín and Candler¹¹ in that it includes K_{eq} . K_{eq} determines the equilibrium mixture composition¹² and τ_c represents the time scale of chemical fluctuations from that composition. q is the RMS magnitude of the fluctuation velocity; a is the speed of sound; u' is the RMS turbulent velocity fluctuation in one direction; $\lambda = \langle u^2 \rangle^{1/2} / \langle (\partial u / \partial x)^2 \rangle^{1/2}$ is the Taylor microscale; $\tau_t = \lambda / u'$ is the turbulent time scale; and Δh^o is the heat of the reaction.

We choose initial $Re_\lambda = 34.5$, $\langle \rho \rangle = 0.5 \text{ kg/m}^3$, and $\langle T \rangle = 3000 \text{ K}$ for N_2 reactions, and $\langle T \rangle = 2000 \text{ K}$ for O_2 reactions. At these initial temperatures, atoms recombine to form molecules and energy is released. Therefore, at time equal zero the reactions are exothermic. We run simulations with all combinations of initial $M_t = 0.35$ and 0.52 , and N_2 or O_2 mass fractions in $[0.0, 0.1, 0.2, \dots, 1.0]$. The total number of simulations performed is forty. The various initial mass fraction conditions lead to distinct evolutions of the nonequilibrium chemistry, and different turbulent flow fields are obtained. During the simulations, the chemical reactions progress and the turbulent kinetic energy decays. Therefore, the values of $\overline{\Delta h^o}$, Da , and M_t vary during the simulations.

SCALING OF TEMPERATURE FLUCTUATIONS

We represent the temperature fluctuations as a PDF,²³ which is calibrated using the results from the DNS. We use histograms and skewness and flatness factors of the temperature fluctuations to obtain the shape of the temperature fluctuation PDF. The shape determines the number of parameters required to generate the distribution. For example, two parameters describe a Gaussian distribution, the mean and the standard deviation. We use the DNS database to find scaling relationships for the PDF parameters in terms of the nondimensional parameters governing the flow, M_t , Da , and $\overline{\Delta h^o}$. During a LES, we would generate the temperature fluctuation PDF using the values of M_t , Da , and $\overline{\Delta h^o}$. Then we would obtain the temperature fluctuations by sampling from this PDF.

For convenience, we choose to look for a distribution of the normalized temperature fluctuations, $T' / \langle T \rangle$, since the DNS predicts zero mean for this distribution. Figure 1 plots the skewness, $S_{T'}$, and flatness, $F_{T'}$, factors of the temperature fluctuations for a typical reacting simulation. After the initial transient ($t / \tau_t > 0.25$), $S_{T'}$ is nearly zero and $F_{T'}$ is

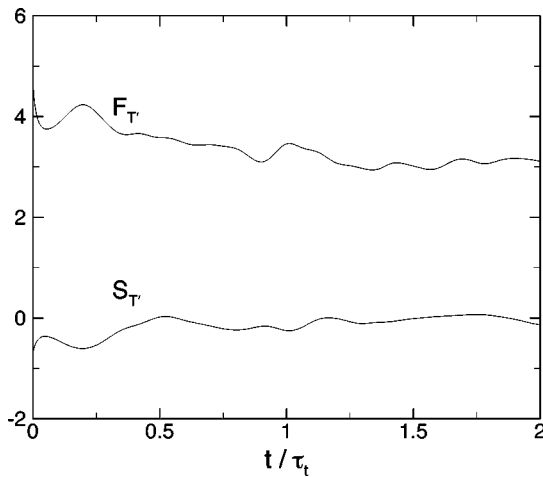


FIG. 1. Time evolution of the skewness, S_T , and flatness, F_T , factors of the temperature fluctuation distribution for N_2 dissociation at initial $M_t = 0.52$ and $\langle c_{N_2} \rangle_0 = 0.3$.

about 3; these values indicate that the temperature fluctuations may be characterized by a Gaussian distribution. Since the mean is zero, we only require the variance, $T'_{RMS}/\langle T \rangle$, to describe the PDF.

The DNS results indicate that $T'_{RMS}/\langle T \rangle$ changes considerably as Da , $\overline{\Delta h^\circ}$, and M_t vary during the simulations. However, for exothermic reactions, when we plot $T'_{RMS}/\langle T \rangle$ versus the relative heat release times a length ratio, λ/l_E , the data (for all combinations of initial mass fractions and turbulent Mach numbers) collapse as shown in Fig. 2. This length ratio is defined from the following relation between the governing parameters:

$$\begin{aligned} \lambda/l_E &= \frac{u' \tau_t}{a \tau_c} \\ &= M_t Da, \end{aligned} \quad (20)$$

where $u' \tau_t = \lambda$ is the distance traveled by a fluid particle moving at the speed of the turbulent intensity. The expansion length l_E is defined as $a \tau_c$, which is the distance traveled by

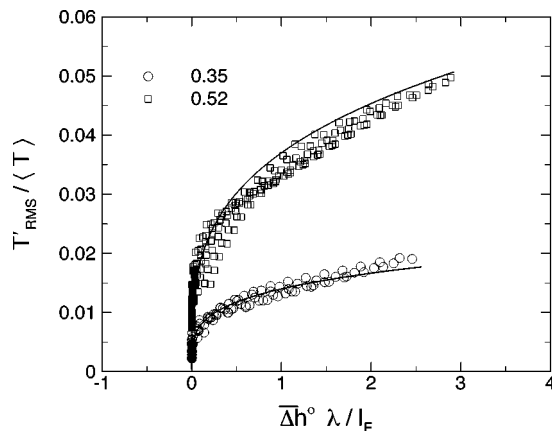


FIG. 2. Standard deviation vs the modulated length ratio, $\overline{\Delta h^\circ} \lambda / l_E$, for N_2 dissociation at initial $M_t = 0.35$ and 0.52 . Filled symbols represent the part of the simulations where the reactions are endothermic. Empty symbols indicate exothermic reactions.

TABLE I. List of constants for $T'_{RMS}/\langle T \rangle = A(\overline{\Delta h^\circ} \lambda / l_E)^B$.

M_t	N_2		O_2	
	A	B	A	B
0.35	0.014	0.250	0.012	0.225
0.52	0.037	0.293	0.028	0.228

acoustic radiation from the chemistry-induced temperature fluctuations. Therefore, λ/l_E represents the ratio of the characteristic distance traveled by a typical particle of fluid to the characteristic distance traveled by the acoustic radiation.

Another way to understand this ratio of length scales is to consider the variation of the strength of the chemistry-turbulence interaction. There is a feedback process for exothermic reactions.¹¹ Namely, a positive temperature fluctuation increases the reaction rate, making the reaction occur more quickly, which releases more heat, further increasing the temperature. However, the feedback process can be weakened by delocalization of the interaction through turbulent motion and motion generated by the local pressure fluctuations (also caused by the interaction). Therefore, in a simplified case where the reaction rate is held constant, the strength of the interaction varies like $(u')^2[(1/u')(1/a)] = u'/a = M_t$. In general, the interaction strength also varies with the reaction rate, or in nondimensional terms, with the Damköhler number. Thus with this argument, we obtain the result shown in Eq. (20).

Under the conditions chosen for our calculations, λ/l_E is always less than one, and as λ/l_E approaches one, $T'_{RMS}/\langle T \rangle$ becomes large, indicating a strong turbulence-chemistry interaction. This occurs when the fluid travels a similar distance as the acoustic radiation induced by the temperature fluctuations. If λ/l_E were larger than one, the interaction would be expected to weaken because the turbulent motion would outrun the acoustic waves produced by the interaction, and the feedback process would be diminished. Also, as λ/l_E approaches zero, the pressure waves outrun the fluid motion and the interaction is weak. Thus, the interaction weakens when λ/l_E departs from 1. In addition, $T'_{RMS}/\langle T \rangle$ is affected by the heat released to the flow,¹¹ and the length ratio must be modulated by $\overline{\Delta h^\circ}$ to give an appropriate relation for the standard deviation. We find that the expression

$$T'_{RMS}/\langle T \rangle = A(\overline{\Delta h^\circ} \lambda / l_E)^B, \quad (21)$$

represents the data, where A and B are constants that depend on the specific reaction. Table I gives the values that have been obtained by fitting Eq. (21) to the DNS results. This power-law fit is shown in Fig. 2 for the N_2 dissociation simulation. As mentioned above, when λ/l_E is greater than one, we would not expect this fit to be valid because it predicts a further strengthening of the interaction.

Moin²⁴ argues that since chemical reactions occur on a molecular scale, the reaction process must be independent of the turbulence length scale. In agreement with this argument, Martín and Candler¹¹ find that the turbulence-chemistry interaction is independent of the Reynolds number for the range of Re_λ that they consider. Thus, it may be surprising

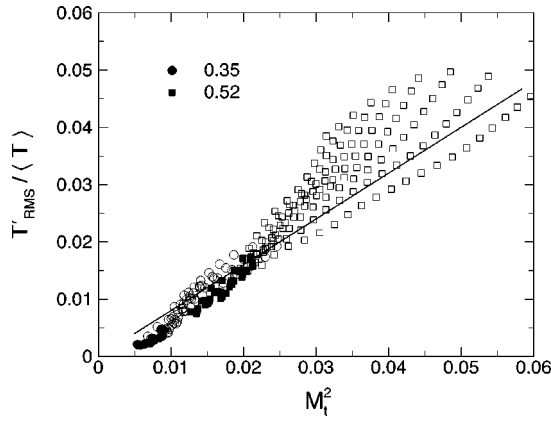


FIG. 3. Standard deviation versus M_t^2 for N_2 dissociation at initial $M_t = 0.35$ and 0.52 . Filled symbols represent the part of the simulations where the reactions are endothermic. Empty symbols indicate exothermic reactions.

that the length ratio gives a relation for $T'_{RMS}/\langle T \rangle$. This occurs because although the reactions are scale independent, their effect on the mean flow depends on the local convective and acoustic scales, and their interaction when the two scales are of the same order of magnitude.

While Eq. (21) and the physically based argument hold for exothermic reactions, the treatment of endothermic reactions must be different. This is reflected in Fig. 2, where the filled symbols indicate the endothermic portion of the simulations. We see that when the reactions become endothermic, the temperature fluctuations are no longer governed by $\overline{\Delta h^0 \lambda} / l_E$. This makes sense physically, because positive temperature fluctuations do not promote further heating of the gas and the feedback process is no longer self-reinforcing.¹¹ Also, when heat is absorbed by the reactions, the gas is cooled, causing an inward-running compression wave. Thus, the acoustic waves no longer delocalize the interaction. In this situation, the strength of the interaction should depend only on the turbulent kinetic energy, $(u')^2$; or in nondimensional terms, $T'_{RMS}/\langle T \rangle \sim M_t^2$.

In agreement with this argument, Fig. 3 shows that $T'_{RMS}/\langle T \rangle$ varies linearly with M_t^2 for the nitrogen simulations for different initial Mach numbers. Note that the empty symbols indicate the exothermic portion of the simulations, and they lie outside the linear fit and do not collapse as in Fig. 2. Thus when the reaction is endothermic, the standard deviation of the PDF of $T'_{RMS}/\langle T \rangle$ may be represented by

$$T'_{RMS}/\langle T \rangle = C M_t^2, \quad (22)$$

where the constant of proportionality, C , is found to be 0.8 for nitrogen dissociation, and 1.0 for oxygen dissociation. Figure 4 shows the variation of $T'_{RMS}/\langle T \rangle$ with $\overline{\Delta h^0 \lambda} / l_E$ and M_t^2 for the oxygen dissociation simulations; we see that the data collapse in the same fashion as in the nitrogen simulations.

A simple single-variable PDF representation of T' gives no distinction between positive or negative temperature fluctuations. Thus, given the PDF for $T'_{RMS}/\langle T \rangle$, we use a conditional sampling to obtain the temperature fluctuations at each point of the flow. Figure 5 shows scatter plots of the

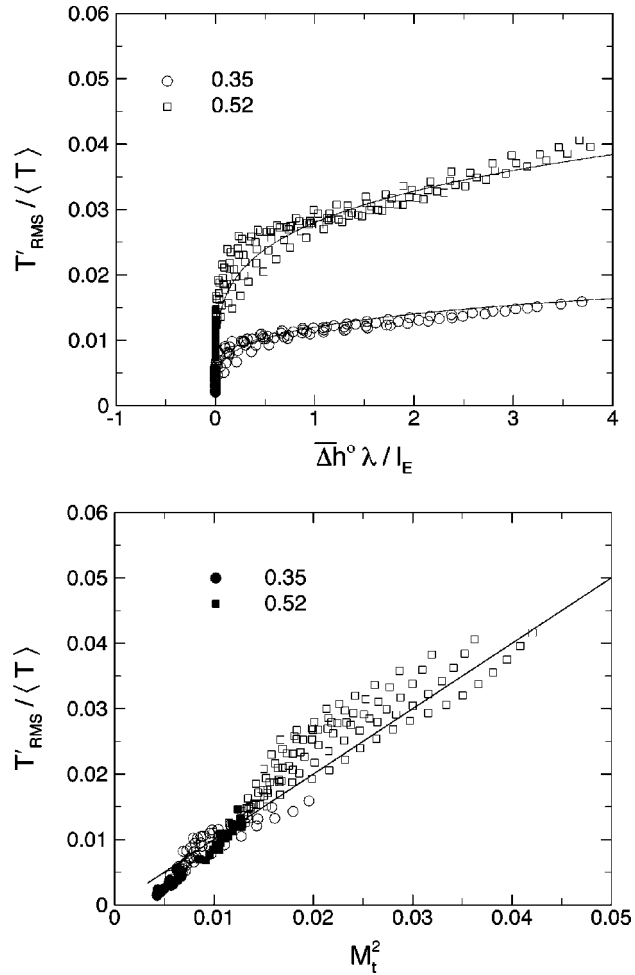


FIG. 4. Standard deviation for O_2 dissociation (a) vs the modulated length ratio, $\overline{\Delta h^0 \lambda} / l_E$; and (b) vs M_t^2 at initial $M_t = 0.35$ and 0.52 . Filled symbols represent the part of the simulations where the reactions are endothermic. Empty symbols indicate exothermic reactions.

temperature fluctuations against the pressure fluctuations, $P'/\langle P \rangle$ at $t/\tau_t = 0.5$ and 2 . We observe that T' is positively correlated with P' for most of the domain during the DNS, indicating that where there is a compression the temperature increases. In our evaluation of the temperature fluctuation model in the next section, we take the sign of T' to be the sign of $P' = \bar{P} - \langle \bar{P} \rangle$, where \bar{P} is the filtered pressure during a LES.

A PRIORI TEST

Being consistent with the data available during a LES, we use the *a priori* test to evaluate the performance of the PDF model. The filtered fields are obtained using a tophat filter given by

$$\bar{f}_i = \frac{1}{2n} \left(f_{i-(n/2)} + 2 \sum_{j=i-(n/2)+1}^{i+(n/2)-1} f_j + f_{i+(n/2)} \right), \quad (23)$$

where f represents a DNS quantity. Various filter widths $\bar{\Delta} = n\Delta$ (where Δ is the grid size and $n = 4, 8, \text{ and } 16$) are used. With these filters, 12%, 30%, and 60%, respectively, of the total turbulent kinetic energy resides in the subgrid scales.

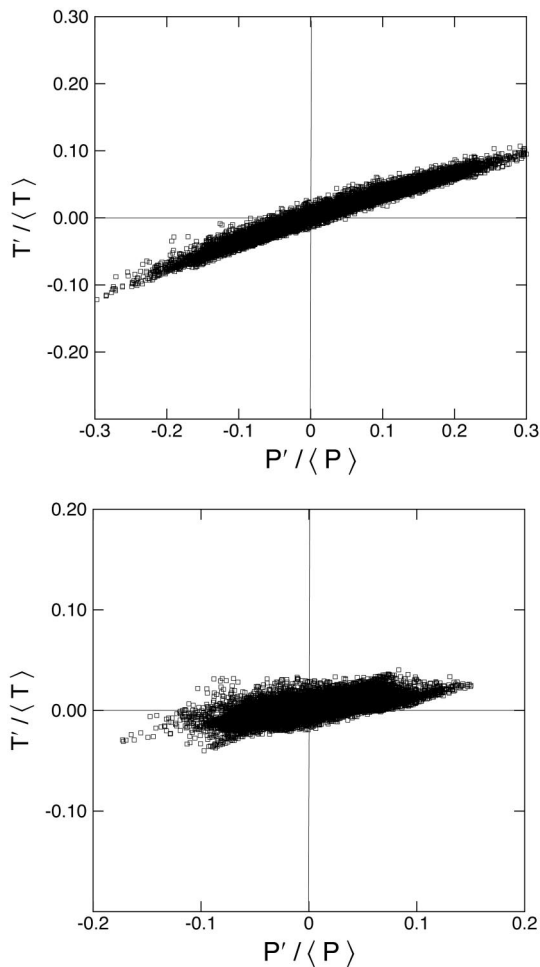


FIG. 5. Scatter plot of the normalized temperature fluctuations, $T'/\langle T \rangle$, and the normalized pressure fluctuations, $P'/\langle P \rangle$, for N_2 dissociation at initial $M_t=0.52$, and $\langle c_{N_2} \rangle_0=0.3$, after (a) $t/\tau_t=0.5$; and (b) $t/\tau_t=2$.

When the turbulence–chemistry interaction is strong the temperature fluctuations are well predicted by Eq. (21) and underpredicted by Eq. (22). The opposite occurs when the interaction is weak. Thus, we compute $T'_{RMS}/\langle \tilde{T} \rangle$ using the largest value given by Eq. (21) or Eq. (22). We evaluate the accuracy of the model by comparing the RMS value of the modeled and DNS fluctuations.

Figure 6 plots the time evolution of T'_{RMS} for nitrogen dissociation with initial $M_t=0.52$ and N_2 mass fraction of 0.3. First consider the DNS result. The initial reaction is exothermic and T'_{RMS} reaches roughly 320 K in less than $0.25t/\tau_t$. The solid triangle indicates where the reaction changes direction and becomes endothermic. Thus, the reaction is exothermic up to nearly $t/\tau_t=1.3$, however, T'_{RMS} decreases rapidly after $t/\tau_t=0.25$. This result can be explained as follows. Although the initial chemical and turbulent time scales are comparable ($Da=0.5$), the Damköhler number decreases rapidly in time. For example, near $t/\tau_t=0.5$ the chemical time scale is over ten times larger than the turbulent time scale. From Eqs. (20) and (21), we see that reducing Da reduces the temperature fluctuations. Thus, the slower chemistry cannot maintain the temperature fluctuations. The temperature fluctuation model predicts nearly cor-

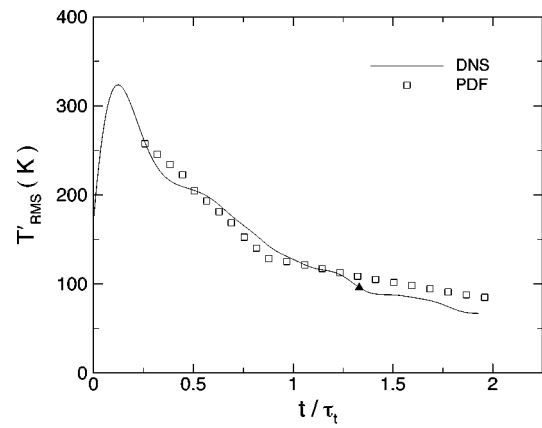


FIG. 6. *A priori* comparison of the RMS temperature fluctuation showing the model performance for N_2 dissociation at initial $M_t=0.52$ and $\langle c_{N_2} \rangle_0=0.3$. The triangle symbol illustrates where the global reaction reverses direction from exothermic to endothermic.

rect RMS amplitudes, except when the reactions are endothermic, in which case the error is up to 30%.

Figure 7 illustrates the effect of filter width on the temperature fluctuation model for this simulation. We observe nearly no dependence of the model on filter width while the reactions are exothermic. This is expected since the exothermic reactions are a scale independent process. However, when the reactions are slow or endothermic, the temperature fluctuations depend mainly on the turbulent motion through the turbulent Mach number. Thus, the prediction of $T'_{RMS}/\langle T \rangle$ given by Eq. (22) deteriorates with increasing filter width as shown in Fig. 7. There are two possible sources of error. First, we have assumed that the constant in Eq. (22) is independent of filter width. Second, we have neglected the contribution of the SGS turbulent kinetic energy to M_t . The second source of error would generate smaller values of T'_{RMS} as the filter width increases. However, we observe the opposite effect in Fig. 7. Thus, the constant in Eq. (22) should depend on filter width.

Finally, Fig. 8 plots the temporal evolution of the average chemical source term evaluated using the DNS temperature and the temperature given by the sum of the average

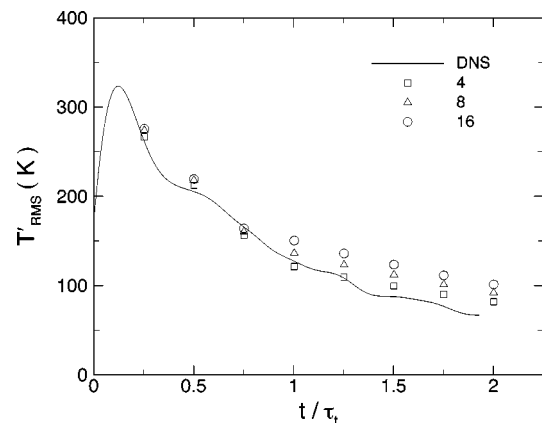


FIG. 7. *A priori* comparison of the RMS temperature fluctuation showing the model performance for various grid filter widths for N_2 dissociation at initial $M_t=0.52$ and $\langle c_{N_2} \rangle_0=0.3$.

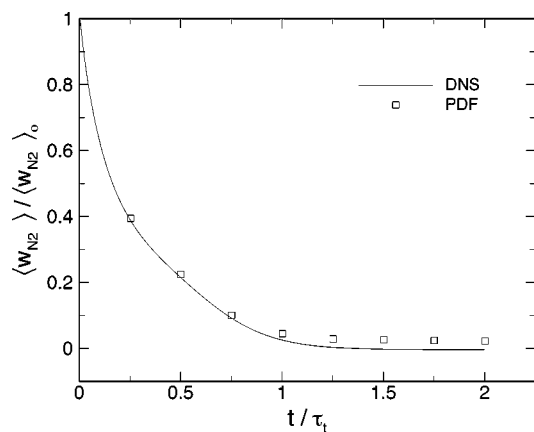


FIG. 8. *A priori* comparison of the nondimensional ensemble average source term showing the performance of the temperature fluctuation model for N_2 dissociation at initial $M_t=0.52$ and $\langle c_{N_2} \rangle_0=0.3$.

temperature and modeled temperature fluctuation. We observe that the slight overprediction of the RMS temperature fluctuation from Fig. 7 results in a slight overprediction of w_{N_2} at later times in the simulation, but the overall agreement is good.

Similar results and model performance are obtained in simulations performed with different initial conditions.

CONCLUSIONS

A probability density-function approach is used to develop a subgrid-scale temperature fluctuation model for the closure of the chemical source term in large-eddy simulations of hypersonic flows. We use a DNS database to calibrate the distribution of $T'/\langle T \rangle$. We find that the distribution is a Gaussian with zero mean and can be described by the standard deviation, $T'_{RMS}/\langle T \rangle$. Exothermic reactions enhance the magnitude of the temperature fluctuations, and the standard deviation can be expressed as $A(\Delta h^\circ \lambda / l_E)^B$. Where λ / l_E is obtained from the nondimensional governing parameters and represents the ratio of the characteristic distance traveled by a fluid particle to the characteristic distance of acoustic radiation. For endothermic reactions, the temperature fluctuations scale linearly with M_t^2 . We find that T' is positively correlated with P' for most of the flow domain. We use this condition to obtain the sign of the modeled temperature fluctuations. We evaluate the model by comparison to DNS and find good agreement. A strong turbulence-chemistry interaction is scale-independent,¹¹ and the model results do not depend on the filter width. However, when the interaction is weak, filtering errors result in an inaccurate prediction of the turbulent Mach number and therefore of the temperature fluctuations.

ACKNOWLEDGMENTS

We would like to acknowledge the support from the Air Force Office of Scientific Research Grant No. AF/F49620-98-1-0035. This work was also sponsored by the Army High Performance Computing Research Center under the auspices

of the Department of the Army, Army Research Laboratory cooperative agreement number DAAH04-95-2-0003/contract number DAAH04-95-C-0008, the content of which does not necessarily reflect the position or the policy of the government, and no official endorsement should be inferred. A portion of the computer time was provided by the University of Minnesota Supercomputing Institute.

¹F. Gao, and E. E. O'Brien, "Direct numerical simulations of reacting flows in homogeneous turbulence," *AIChE. J.* **37**, 1459 (1991).

²R. L. Gaffney, J. A. White, and J. P. Drummond, "Modeling turbulence-chemistry interactions using assumed PDF methods," *AIAA Paper No. 92-3638* (1992).

³S. H. Frankel, V. Adumitroaie, C. K. Madnia, and P. Givi, "Large eddy simulation of turbulent reacting flows by assumed PDF methods," *FED-Engineering Applications of Large Eddy Simulations, ASME* **162**, 81 (1993).

⁴A. W. Cook and J. J. Riley, "A subgrid model for equilibrium chemistry in turbulent flows," *Phys. Fluids* **6**, 2868 (1994).

⁵C. Dopazo and L. Valiño, "PDF approach and stochastic models of the turbulent mixing of inert and reactive statistically homogeneous scalar fields," *Transp. Theory Stat. Phys.* **23**, 339 (1994).

⁶P. Givi, V. Adumitroaie, G. J. Sabini, and G. S. Shieh, "LES, DNS and RANS for the analysis of high-speed turbulent reacting flows," *NASA-CR-196822* (1994).

⁷R. L. Gaffney, J. A. White, S. S. Girimaji, and J. P. Drummond, "Modeling temperature and species fluctuations in turbulent, reacting flows," *Comput. Syst. Eng.* **5**, 117 (1994).

⁸A. W. Cook, J. J. Riley, and G. Kosàly, "A laminar flamelet approach to subgrid-scale chemistry in turbulent flows," *Combust. Flame* **109**, 332 (1997).

⁹P. A. Nooren, H. A. Wouters, T. W. J. Peeters, D. Roekaerts, U. Maas, and D. Schmidt, "Monte Carlo PDF modelling of a turbulent natural-gas diffusion flame," *Combust. Theor. Modelling* **1**, 79 (1997).

¹⁰C. D. Pierce and P. Moin, "Large eddy simulation of a confined coaxial jet with swirl and heat release," *AIAA Paper No. 98-2892* (1998).

¹¹M. P. Martín and G. V. Candler, "Effect of chemical reactions on decaying isotropic turbulence," *Phys. Fluids* **10**, 7 (1998).

¹²R. N. Gupta, J. M. Yos, R. A. Thompson, and K. Lee, "A review of reaction rates and thermodynamic and transport properties for an 11-species air model for chemical and thermal nonequilibrium calculations to 30 000 K," *NASA-RP-1232* (1990).

¹³M. Germano, U. Piomelli, P. Moin, and W. H. Cabot, "A dynamic subgrid-scale eddy viscosity model," *Phys. Fluids A* **3**, 1760 (1991).

¹⁴D. K. Lilly, "A proposed modification of the Germano subgrid-scale closure method," *Phys. Fluids A* **4**, 633 (1992).

¹⁵P. Moin, K. Squires, W. Cabot, and S. Lee, "A dynamic subgrid-scale model for compressible turbulence and scalar transport," *Phys. Fluids A* **3**, 2746 (1991).

¹⁶E. T. Spyropoulos and G. A. Blaisdell, "Evaluation of the dynamic model for simulations of compressible decaying isotropic turbulence," *AIAA J.* **34**, 990 (1996).

¹⁷S. Ghosal, T. S. Lund, P. Moin, and K. Akselvoll, "A dynamic localization model for large-eddy simulation of turbulent flows," *J. Fluid Mech.* **286**, 229 (1995).

¹⁸F. Gao and E. E. O'Brien, "A large-eddy simulation scheme for turbulent reacting flows," *Phys. Fluids A* **5**, 1282 (1993).

¹⁹J. Réveillon and L. Vervisch, "Response of the dynamic LES model to heat release induced effects," *Phys. Fluids* **8**, 2248 (1996).

²⁰M. P. Martín, U. Piomelli, and G. V. Candler, "Subgrid-scale models for compressible LES," *Proceedings of the 1999 ASME Symposium on Transitional and Turbulent Compressible Flow* (1999).

²¹S. K. Lele, "Compact finite difference scheme with spectral-like resolution," *J. Comput. Phys.* **103**, 16 (1992).

²²J. R. Ristorcelli and G. A. Blaisdell, "Consistent initial conditions for the DNS of compressible turbulence," *Phys. Fluids* **9**, 4 (1997).

²³S. B. Pope, "PDF methods for turbulent reactive flows," *Prog. Energy Combust. Sci.* **11**, 119 (1985).

²⁴P. Moin, "Progress in large eddy simulation of turbulent flows," *AIAA Paper No. 97-0749* (1997).